A COMPUTATIONAL STUDY TO PREDICT THE COMBINED EFFECTS OF SURFACE ROUGHNESS AND HEAT FLUX CONDITIONS ON CONVERGING-NOZZLE FLOWS

A. Alper OZALP
Department of Mechanical Engineering, Uludag University, 16059 Gorukle Bursa, TURKEY
Contact: aozalp@uludag.edu.tr, Web : http://www.geocities.com/aaozalp/

Received June 2004, Accepted January 2005
No. 04-CSME-20, E.I.C. Accession 2810

Abstract

Critical design parameters on the performance prediction of converging nozzles are the geometric features and the operating conditions, which include the stagnant properties at the inlet, frictional and heat transfer behaviors on the nozzle wall; where the latter two are hard to handle together in compressible high-speed flows. This paper presents a recent computational model, that integrates the axisymmetric continuity, momentum and energy equations, to predict the combined effects of surface roughness and heat flux conditions on the flow and heat transfer characteristics of compressible flows through converging nozzles. To build a comprehensive overview, analyses are conducted at convergence half angles from 0^o to 9^o and inlet stagnation to back pressure ratios ranged from 1.01 to 2, covering both the un-choked and choked cases. Non-dimensional surface roughness and surface heat flux values are in the order of 0.0025-0.05 and 20-2000 kW/m^2 respectively. The influences of the model parameters on the nozzle performance are discussed through the streamwise variations of Mach number, shear stress, discharge coefficient and Nusselt number; to verify the validity of the model comparisons are made with the numerical and experimental data available in the literature.

UNE ETUDE D'EVALUATION POUR DETERMINER LES EFFETS COMPOSES DE LA RUDESSE DE SURFACE ET DES CONDITIONS DE FLUX DE CHALEUR SUR LES LANCES CONVERGEANTES

Résumé

Les paramètres de conception critique sur la performance de détermination des lances convergentes sont des caractéristiques géométriques et des conditions de travail qui comprennent les propriétés stagnantes à l'ouverture et les conduites de friction et de transfert de chaleur sur le mur de lance, et il est difficile d'étudier, en particulier, les deux dernières constructions ensemble dans les circulations à grande vitesse compressibles. Cet article présente un nouveau modèle d'évaluation utilisant la continuité axisymétrique, les équations de moment et d'énergie en même temps pour déterminer les effets composés de la rudesse de surface et des conditions de flux de chaleur sur la circulation et les propriétés de transfert de chaleur de la circulation compressible à travers les lances convergentes. Pour construire une opinion détaillée, les analyses ont été effectuées sur une convergence à demi-angle changeant de 0 à 9 degré et la stagnation à l'ouverture et le taux de pression à la sortie ont varié de 1.01 à 2 de façon à comprendre les cas bouchés et débouchés. La rudesse de surface sans dimensions et les valeurs de flux de chaleur sur la surface étaient dans l'ordre de 0.0025-0.05 et 20-2000 kW/m^2 respectivement. L'influence des paramètres de modèle sur la performance de lance a été discutée avec les variations de nombre de Mach dans la direction de flux et les variations de tension de torde, de coefficient de décharge et de nombre de Nusselt. Pour vérifier la validité du modèle, on a fait des comparaisons par les données numériques et expérimentales présentes dans la littérature.

1. INTRODUCTION

Nozzles, as a downstream component of a complete running assembly, can be encountered in a wide variety of engineering applications. A nozzle can be the essential part of the exhaust system of nuclear propulsion engines [1], which utilize fusion reactions to generate energy and thrust, it can also be the flow accelerator in environmental control systems of commercial aircrafts [2], that supplies fresh air at certain temperature and pressure to the passenger cabin. Regardless of the objective, the accurate prediction in design-oriented calculations of compressible nozzle flows is still a challenging task for the aerodynamicist and achieves increasing importance when the nozzle performance is significantly influenced by geometry, inlet conditions and sources of non-isentropic character.

Many experimental and numerical works reported information on nozzle performance, flow and heat transfer characteristics with various inlet-boundary conditions and flow geometries. Instabilities in the propulsion of rockets, due to pressure and temperature fluctuations at the upstream of rocket nozzle and the flow geometry, were numerically considered by Assovskii and Rashkovskii [3]. Massier et al. [4] conducted experiments in a 10^o convergence half angle nozzle with different working fluids and with a wide range of inlet stagnation pressures and recorded lower discharge coefficients with the decrease of inlet stagnation pressure. Krueger and Gharib [5] experimentally investigated the effects of nozzle exit over-pressure on vortex formation with its contribution to nozzle thrust. Park et al. [6] investigated sonic nozzles that are applied to gas flow-rate measurements and determined that the critical pressure ratio is highly dependent on the Reynolds number rather than area ratio especially in the cases with low flow velocity. Kim et al. [7] considered several kinds of gases and turbulence models with a wide range of Reynolds numbers on different sonic nozzle geometries. Variation of discharge coefficients for sonic nozzles with flow geometry and Reynolds number was reported by Paik et al. [8], who determined higher discharge coefficients with the increase of mass flow rate. Lear et al. [9] modeled dissipative effects of heat transfer on the exit kinetic energy and on nozzle efficiency and determined significant losses in efficiency due to heat transfer especially when the ratio of the inlet stagnation to back pressure converge to unity. Ribault and Friedrich [10] implemented the turbulent momentum and heat transport analogies in a code and investigated the behavior of compressible flow along adiabatic and cooled walls. Orieux et al. [11] illustrated steady and transient performance of micro-nozzles for various nozzle geometries, ambient conditions and surface cooling, where thrust values decreased both with cooling and with narrower nozzle exit. Sato et al. [12] presented the recent data of a real time propulsion ramjet engine, which is equipped with the air-cooling system. Back et al. [13] performed an experimental investigation of gas dynamics and heat transfer in a choked nozzle with cooling. Ahmad [14] correlated the variation of nozzle discharge coefficients and surface heat transfer values for nozzle flows and Bartz [15] handled the heat transfer phenomena in compressible nozzle flows and considered Nusselt number as a function of inlet stagnation pressure and convergence half angle.

In addition to the geometric studies, inlet/exit conditions and heating/cooling applications on nozzles, the existence of surface roughness (ε) at the flow surface is becoming a major interest for compressible and incompressible nozzle flows. The main sources of augmentations in the surface roughness values are high pressure and temperature inside the nozzle and gas-solid particle flows especially in the exhaust systems of aero/industrial gas turbines and rockets. Maisonneuve [16] showed that the surface roughness of real nozzles grows exponentially with increasing temperature. Real time data of Ariane 5 rocket is presented by Bussiere and Mora [17], where the relative roughness (ε/D) of the booster nozzle is increased from perfect surface finish to 0.012 during a flight, that initiates with launch and ends at the orbit. Shipway [18] investigated the erosion and wear characteristics of exhaust nozzles, exposed to accelerated solid particles with various sizes and trajectory directions, and recorded an increase in relative roughness data up to 0.024. An experimental study on nozzle wear due to gas-solid particle flow was also carried out by Kumar et al. [19], who established an increase in relative roughness values from 0.006 to 0.052. Krishnan et al. [20] performed an electron microscope investigation on wear patterns of agricultural sprayer nozzles,

operating at inlet to back pressure ratios of 1.37-5.51 and determined that the relative roughness values attained the range of 0.02-0.04.

The available literature deal either with the cooling or constant surface temperature investigations however combined effects of surface roughness and heating on compressible flows is not considered. The objective of the present study is to present a new mathematical model, capable of performing comprehensive compressible converging-nozzle flow analysis including the implementation of both surface roughness (ε) and surface heat flux (Q) conditions. Isentropic and non-isentropic computations are carried for flows in un-choked and choked nozzles for various convergence half angles (α), inlet stagnation to back pressure ratios (β), Q and ε cases. The model is validated with previous experimental and numerical results and the combined effects of Q and ε on the flow and heat transfer characteristics are discussed in detail.

2. NUMERICAL ANALYSIS

2.1 Modelling

The overall aim is to build a predictive model for converging-nozzle flows in the presence of surface roughness and constant heat flux conditions. The model should permit the determination of necessary design parameters such as nozzle geometry, inlet-boundary conditions for any given performance requirement depending on the applications, thus the main requirements are adaptability, simplicity and low calculation time. The calculations rely on the principles of mass and energy conservation and on the momentum and state equations applied to the control volume, given in Figure 1. It is assumed that the stagnation conditions of pressure and temperature in the storage tank, upstream of the converging nozzle, are homogeneous and, as in many numerical work [1, 6, 9, 11], air is considered as an ideal gas with a compressibility factor of 1 and the air velocity, pressure and temperature are taken as uniform across any section normal to the flow axis. Since air properties, like specific heat at constant pressure (C_p), kinematic viscosity (ν) and Prandtl number (Pr), are substantially dependent on temperature [21], they are characterized by 6^{th} order polynomials with an uncertainty of less than 0.02% and the temperature dependency is indicated by the superscript T throughout the formulation.

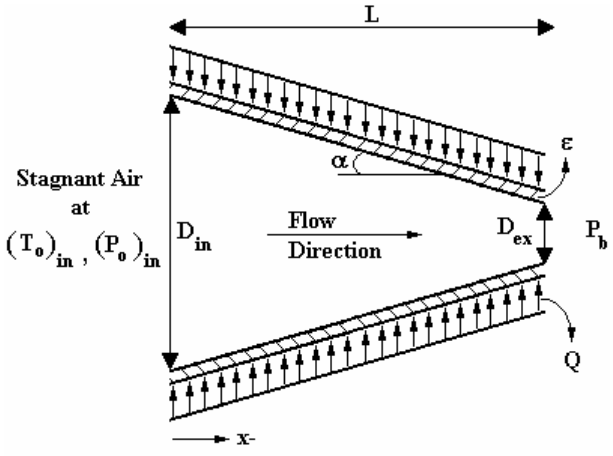

Figure 1. Nozzle outline.

As the work is interested in flows with friction and heat transfer, stagnation properties will also vary in the flow direction, thus the conventional equations (Eqs. 1(a-b)) for compressible, isentropic and one-dimensional flows are applicable only with the simultaneous handling of the momentum and energy equations.

$$\frac{(P_o)_i}{P_i} = \left(1 + \frac{\gamma - 1}{2} M_i^2\right)^{\frac{\gamma}{\gamma-1}} \qquad \frac{(T_o)_i}{T_i} = 1 + \frac{\gamma - 1}{2} M_i^2 \qquad \text{(1a-b)}$$

The nodal values of air velocity (U), density (ρ) and mass flow rate ($\dot{m}$) can be calculated by Eqs. 2(a-c), where $\dot{m}$, being the most significant consideration from numerical point of view, is kept constant in the flow direction. On the other hand Reynolds number (Eq. 2(d)) is assigned to each differential cell with the mean cellular values of U, D and ν.

$$U_i = M_i \sqrt{\gamma R T_i} \qquad \rho_i = \frac{P_i}{R T_i} \qquad \dot{m} = \rho_i U_i A_i \qquad (Re_D)_n = \frac{\overline{U_n}\,\overline{D_n}}{\overline{\upsilon_n^T}} \qquad \text{(2a-d)}$$

The friction factor (Eq. 3(a)) is computed for each cell, within the flow volume, with the local values of $(Re_D)_n$ and $\varepsilon/\overline{D_n}$, and the cell based shear stress (τ) and friction force (F_f) can be expressed with Eqs. 3(b-c).

$$\frac{1}{\sqrt{f_n}} = -3.6 \log\left[\frac{6.9}{(Re_D)_n} + \left(\frac{\varepsilon/\overline{D_n}}{3.7}\right)^{1.11}\right] \qquad \tau_n = \overline{f_n}\,\overline{\rho_n}\,\frac{\left(\overline{U_n}\right)^2}{2} \qquad (F_f)_n = \tau_n \pi \overline{D_n} \Delta x_n \qquad \text{(3a-c)}$$

The one-dimensional momentum (Eq. 4) and energy equations (Eq. 5(a)) are applied to each differential cell in the nozzle, where the nodal properties such as P, U and C_p are interrelated with the contributions of cellular variants like F_f, I and dq. Eq. 5(a) represents conservation of mechanical and thermal energy by the implementation of cell based surface flux (Eq. 5(b)) and the frictional loss term.

$$P_i A_i + \dot{m} U_i = P_{i+1} A_{i+1} + \dot{m} U_{i+1} + (F_f)_n + I_n \qquad (4)$$

$$(C_P^T)_i T_i + \frac{U_i^2}{2} + (dq)_n = (C_P^T)_{i+1} T_{i+1} + \frac{U_{i+1}^2}{2} + \frac{(F_f)_n \overline{U_n}}{\dot{m}} \qquad (dq)_n = \frac{Q(A_s)_n}{\dot{m}} \qquad \text{(5a-b)}$$

Vargas and Bejan [2] evaluated the heat transfer data in their mathematical model for a converging-nozzle flow, where the Mach number was in the range of 0.50-0.85, with the empirical correlation of Eq. 6(a). In the current work the Mach numbers are within 0.15-1.0, similar to the subsonic data of [2], and Eq. 6(a) is applied with the cell-based values of f, Pr and Re_D. Moreover the combined effects of ε and Q on $\dot{m}$ are investigated through the non-dimensional discharge coefficient (C_d) of Eq. 6(b), which compares the real $\dot{m}$ with that of the isentropic case.

$$(Nu_D)_n = \frac{\left(\overline{f_n}/2\right)\left[(Re_D)_n - 10^3\right]\overline{Pr_n^T}}{1 + 12.7\left(\overline{f_n}/2\right)^{0.5}\left[\left(\overline{Pr_n^T}\right)^{2/3} - 1\right]} \qquad C_d = \frac{\dot{m}_{real}}{\dot{m}_{isen}} \qquad \text{(6a-b)}$$

2.2 Computation

For the one-dimensional, compressible marching procedure, forward difference discretization is applied in the flow direction, as defined by Chapra and Canale [22]. Since the continuity, momentum and energy equations are to be solved in harmony, the geometric domain is divided into n sequential cells, having an equal width of Δx. The fineness of the computational grids is examined to ensure that the obtained solutions are independent of the grid employed. Initial runs indicated that beyond 1000 cells the results showed no sign of change with grid density, thus to provide more reasonable predictions computations are performed with n=1000. Flow parameters, like U, P, T, ρ and stagnation data (P_o, T_o), are calculated at the nodes of these cells, that are numbered from i=1 to n+1, whereas τ, I, Re_D and Nu_D are evaluated on cell basis using the mean values of nodal inlet and exit data of each cell.

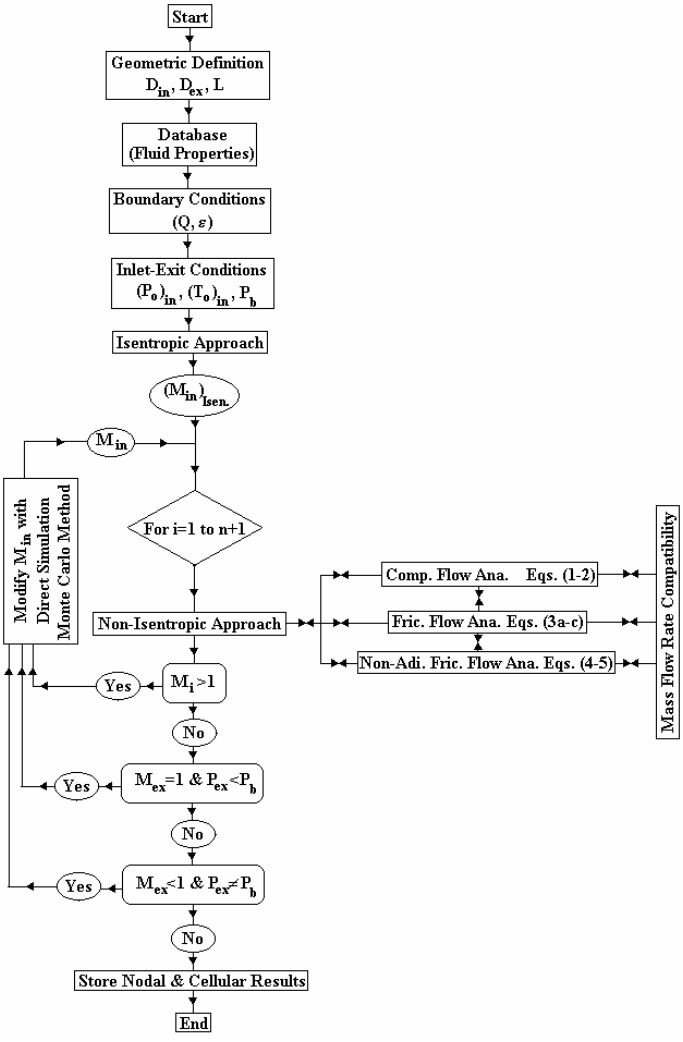

Figure 2. Flowchart of the numerical procedure for non-adiabatic & frictional compressible flow.

As given in Figure 2, by disregarding the surface roughness and heat transfer, the flow of the solution logic first handles the problem as of isentropic type, which is easy to manipulate as described by Laney [23]. The M_{in} value of the isentropic approach is the initial guess of the iterative solution procedure of the non-isentropic nozzle flow. The non-isentropic approach governs the complete equation set described above however if the solution scheme encounters singularities, like M_i>1,

$M_{ex}=1$ & $P_{ex}<P_b$ or $M_{ex}<1$ & $P_{ex}\neq P_b$, M_{in} is modified by direct simulation Monte Carlo method, similar to that explained by Wu and Tseng [24]. The convergence criteria for $\dot{m}$ throughout the flow volume is in the order of 0.01% and successive non-isentropic runs are performed until the M_{ex} is in the range of 0.99-1.0 for the choked nozzle, and the shift of P_{ex} from the back pressure is less than $P_b x10^{-4}$ for the un-choked case.

3. RESULTS AND DISCUSSION

Numerical investigations are carried out with the nozzle convergence half angles of $\alpha=0^o$, 3^o, 6^o and 9^o, with inlet stagnation pressure values $(P_o)_{in}$=101, 125, 150, 175 and 200 kPa, corresponding to $\beta=(P_o)_{in}/P_b$ range of 1.01 to 2, where back pressure (P_b) is fixed to 100 kPa. Influence of the constant surface roughness on the flow and heat transfer characteristics is simulated by applying 5 different non-dimensional cases of ε/D_{in}=0.0025, 0.0125, 0.025, 0.0375 and 0.05; moreover the effects of constant surface heat flux are evaluated by imposing 6 distinct values of Q=20, 400, 800, 1200, 1600 and 2000 kW/m^2. Results are discussed through streamwise variations of Mach number, shear stress, discharge coefficient and Nusselt number.

3.1 Flow Characteristics

Variations in the streamwise M are given in terms of β, α and Q-ε in Figures 3(a)-(b) respectively. It can be seen from Figure 3(a) that flows with lower β result in lower M_{in} and M_{ex} for all nozzle convergence half angles ($\alpha=0^o$-9^o). When compared with β=2 pattern, β=1.50 caused a decrease of 16% and 14% in M_{in} for the isentropic and Q=2000 kW/m^2 cases in the $\alpha=0^o$ nozzle, whereas the similar ratios for β=1.25 are 38% and 35%. On the other hand for the $\alpha=9^o$ nozzle, the decrease amounts in M_{in} for β=1.50 are 4.6% and 9%, and for β=1.25 are 19% and 26% for the isentropic and Q=2000 kW/m^2 cases respectively. These proportions put forward that the decrease amounts are more apparent for lower α and less evident for sharp convergent cases. In the downstream section M_{ex} values are identical and equal to 1, being independent of M_{in}, for the β=2 case, since $(P_o)_{in}$=200 kPa corresponds to choking condition for the complete α range. However as β is lowered, the nozzles run at un-choked condition with accompanied decreases in M_{ex}. The variations in M_{ex}, when compared with the above discussions on M_{in}, are small and kept in the range of 2%-4% for the complete α, Q and β set.

Figure 3(a) further implies that application of surface heat flux produces lower M values throughout the nozzle, regardless of the level of β and α. These findings are similar to those of Lear et al.'s [9] numerical and Sato et al.'s [12] experimental determinations. Application of the constant surface temperature condition on the nozzle wall [9] caused flow velocities, thus M, to decrease, whereas the cooling of the nozzle surface [12], which is the counter operation of the present work-focus, resulted in higher mass flow rates. For $\alpha=0^o$ nozzle the heat flux of Q=2000 kW/m^2 results in a decrease in M_{in} of 23%, 20.7% and 18.8% for β of 2, 1.50 and 1.25 respectively. On the other hand the same flux constitutes lower M_{in} by 8.3%, 12.6% and 15.9% for $\alpha=9^o$ in the same β range. These proportions suggest that effect of heat flux on M pattern is more apparent with lower α. Nevertheless, as the influence of Q on M decreased with lower β for $\alpha=0^o$, the contrary outcome exists for $\alpha=9^o$ which reveals the combined decreasing effects of Q and α on M variation.

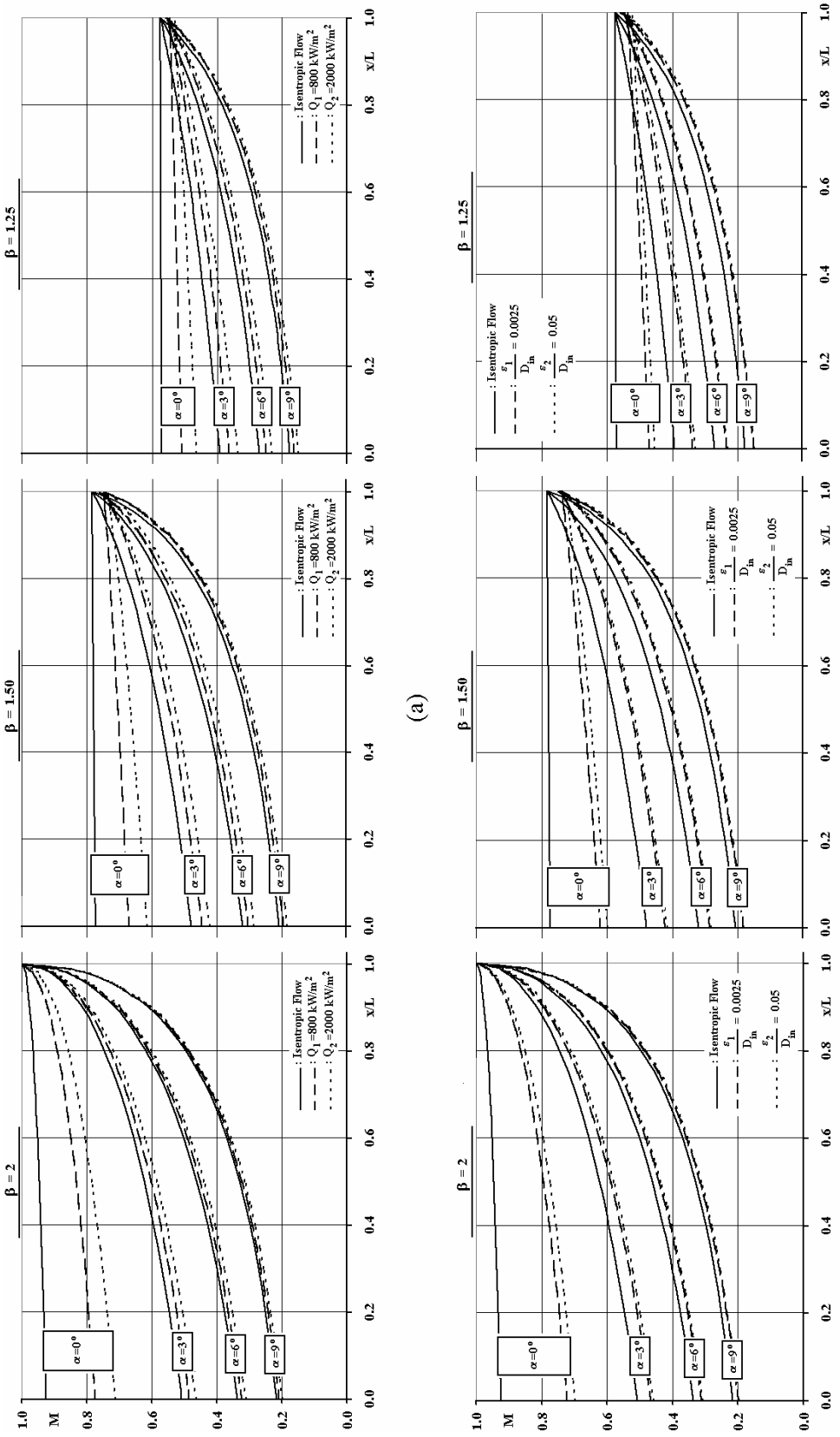

Figure 3. Influence of (a) constant heat flux and (b) surface roughness conditions on streamwise Mach number variations.

Effects of various surface roughness cases on M are compared within each other and with the isentropic flow in Figure 3(b). As in the heat flux discussions, surface roughness produces lower M values, thus mass flow rates, for all β and α cases. The application of the non-dimensional surface roughness of ε/D_{in}=0.0025 to the $\alpha=0^o$ nozzle resulted in lower M_{in} by 17.9%, 19.8% and 21.9% for the β of 1.25, 1.50 and 2 respectively, where else the corresponding decrease rates for ε/D_{in}=0.05 are 20.7%, 22.6% and 24.4%. On the other hand for the nozzle with the sharpest convergence half angle ($\alpha=9^o$) indicated decrease amounts of 15.9%, 11.6% and 7.83% for ε/D_{in}=0.0025 and 17.6%, 13.0% and 9.2% for ε/D_{in}=0.05 with the β of 1.25, 1.50 and 2 respectively. It is obvious that the reduction amounts for the lowest and highest roughness cases are close, indicating that ε itself, whether small or big, is a resistive cause for gas motion even at high velocities of 0.15<M<1.0. Moreover the divergence of the decrease rates, among the two ε/D_{in} cases, become smaller as α is increased; which puts forward that α is more dominant, than ε, on Mach number pattern. On the other hand, similar to the heat flux discussion, it can be seen that the decrease rates increase with higher β for the $\alpha=0^o$ nozzle, whereas the opposite is the outcome for the $\alpha=9^o$ case, revealing the combined effect of ε and α.

Shear stress variations, evaluated at constant Q values of 20, 800 and 2000 kW/m^2, with constant ε/D_{in}=0.0125 are presented in Figure 4(a). Lower β, higher α and Q caused τ values to decrease, especially, at the upstream nozzle sections. Ribault and Friedrich [10] reported higher f values with surface cooling which is in harmony with the present findings. From the definition of shear stress (Eq. 3(b)), the above defined reducing effects of higher α and Q and lower $(P_o)_{in}$ on M and $\dot{m}$ values explain the lower values of τ beginning at the inlet section of the nozzles. However the decrease rates of τ becomes smaller with higher β values for the complete α range. Moreover towards downstream, the τ values of the higher α cases exceed those of the nozzles with smaller α, which can be clarified by inspecting the variations of velocity, density and temperature values of the flowing air towards the τ intersection area. Towards the onset of the intersection area the difference of Mach numbers gets smaller (Figure 3), ρ and T values of the higher α cases exceeds those of the smaller α by 10-18% and 10-70 ^{o}C respectively. Increase of air viscosity with temperature and together with the augmentations in M and ρ data contributes the enhancement of sharp narrowing nozzle's τ data. On the other hand the locus of the intersection points of τ curves are in the x/L range of 0.87-0.96, 0.92-0.98 and 0.97-0.98 for β values of 1.25, 1.50 and 2 respectively. These records show that as inlet stagnation pressure is increased the intersection range becomes narrower and moves downstream.

Figure 4(b) presents ε effects on τ distributions for various α and β cases. As expected, higher ε/D_{in} resulted in higher τ values in the complete α and β set. On the other hand independent of β, τ_{in} values, evaluated for ε/D_{in} of 0.0025 and 0.025, are separated by a factor of 2.06 for $\alpha=0^o$ and 2.09 for $\alpha=9^o$, whereas at the exit the ratios become 2.10 and 2.27 for $\alpha=0^o$ and $\alpha=9^o$ respectively. It is obvious that the proportions increase with both convergence half angle and streamwise direction, which is an outcome of the above described increase of density and flow temperature values in x-direction and with higher α. In addition, the exit to inlet τ ratios are in the range of 1.21-1.40 for $\alpha=0^o$ and 12.9-16.31 for $\alpha=9^o$, where the lower and upper limits correspond to β of 1.25 and 2 respectively. These findings put forward that as α and β increases, the downstream nozzle walls will be exposed to augmented local friction and flow temperature.

Combined effects of α, β and Q on the discharge coefficient are given in Figure 5(a), with the constant value of ε/D_{in}=0.0125. Higher β values resulted in higher C_d for the complete α and Q ranges, which indicates that β is the dominant parameter on C_d. Also Park et al. [6], in their experimental work, and Ahmad [14], in his numerical investigation, determined augmented C_d with higher β. Moreover α plays the contrary role of β and decreases C_d, where similar findings were also reported by Kim et al. [7]. Kim et al. [7] also indicated that the effect of α on C_d increases with the decrease of β.

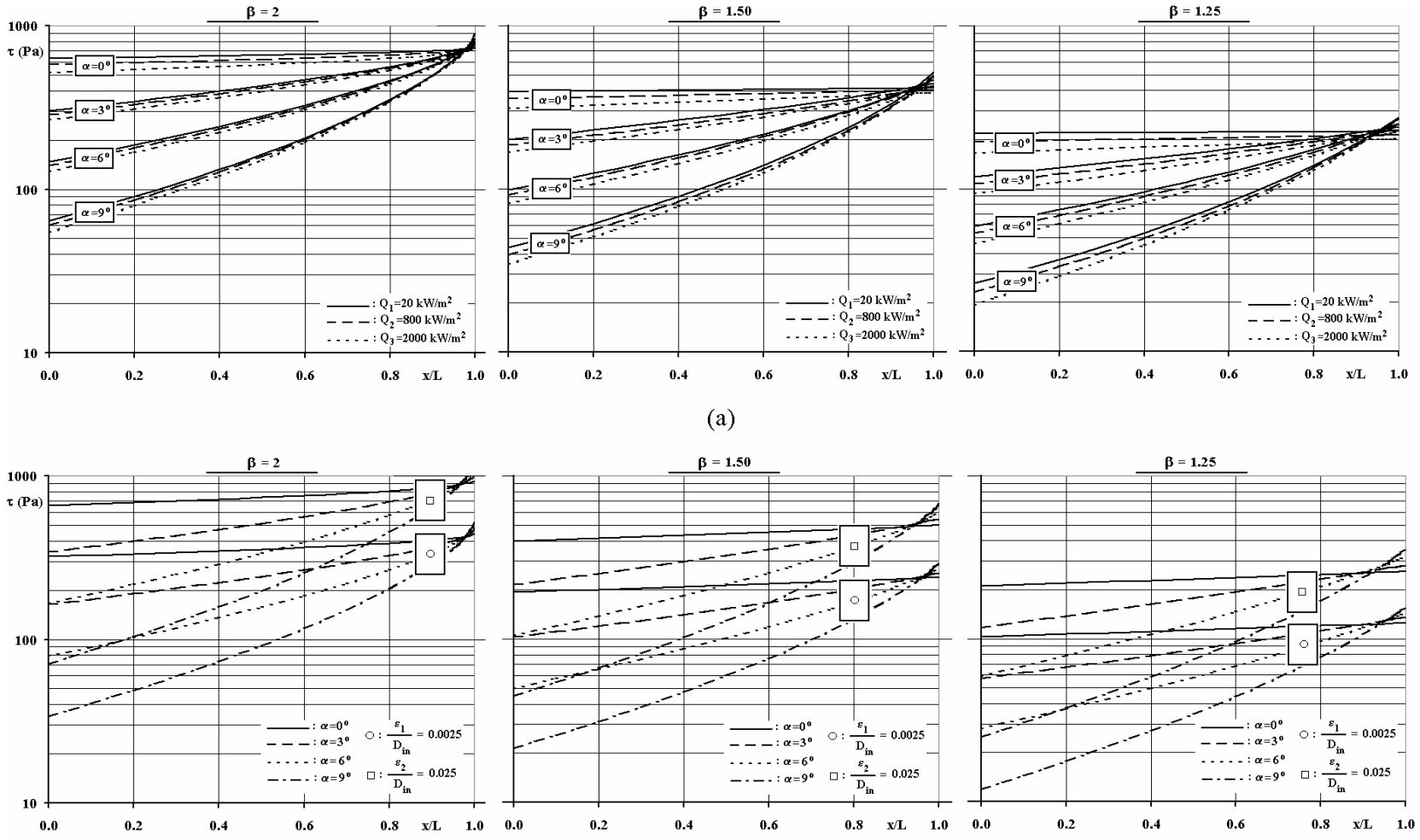

Figure 4. Influence of (a) constant heat flux and (b) surface roughness conditions on streamwise shear stress variations.

Our numerical results show, particularly for the Q=2000 kW/m^2 case, that as $\alpha=0^o$ yielded C_d of 0.93, 0.87 and 0.53 for β=2, 1.25 and 1.01 respectively, the similar values of $\alpha=9^o$ are 0.92, 0.84 and 0.48 for the same β range. These records are in harmony with the findings of [7] and point out the decrease in C_d with α as well. Like α, application of Q decreased the C_d, which contributes to M variations with Q (Figure 3(a)) and show parallelism with the reports of Paik et al. [8], who correlated C_d with respect to Re_D and found out a direct proportion. However when compared with α, Q is more effective on C_d, which can be clarified by the above decrease rates where the maximum gap is just 0.05 among the cases of $\alpha=0^o$-β=1.01 and $\alpha=9^o$-β=1.01. Figure 5(a) further implies that for the neglectable Q of 20 kW/m^2, C_d values converge to the 0.97-0.99 interval, which is congenial with experimental reports of Massier et al. [4] and Kim et al. [7], who carried out their investigations with adiabatic nozzle walls.

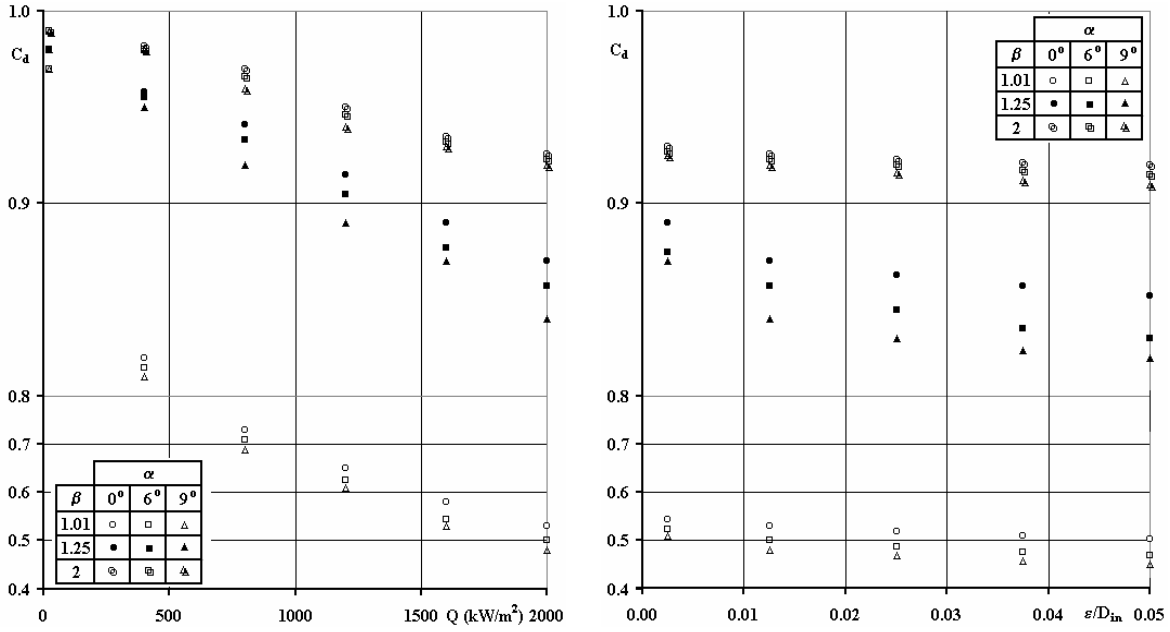

(a) (b)

Figure 5. Influence of (a) constant heat flux and (b) surface roughness conditions on nozzle discharge coefficient.

Surface roughness effects on C_d, with various β and α, are discussed in Figure 5(b), where the numerical analysis are carried with Q=2000 kW/m^2 are presented only. The decrease of C_d with higher ε/D_{in} is common for all β, however the effect of roughness is more noteworthy in lower β values. For the $\alpha=0^o$-β=2 case, the difference in C_d among the ε/D_{in}=0.0025 and ε/D_{in}=0.05 cases is 0.01, whereas the corresponding difference increases to 0.042 in the system of $\alpha=0^o$-β=1.01. As discussed in Figure 3, lower M and lower $\dot{m}$ are the natural outcomes of decreased β, thus these records indicate that ε is more influential on C_d with the systems having lower $\dot{m}$. As the convergence half angle is increased to $\alpha=9^o$, the gap in C_d, among the lowest and highest roughness parameters, is evaluated as 0.016 and 0.059 for the β of 2 and 1.01 respectively. These records put forward the combined decreasing consequences of ε and α on C_d, moreover, from the extreme effects point of view, surface roughness and convergence half angle individually result in same amount of variation on the nozzle discharge coefficient.

3.2 Heat Transfer Characteristics

Streamwise Nu_D variations are evaluated for different α and β cases, by applying constant surface heat flux values of 20, 800 and 2000 kW/m^2, with the constant value of ε/D_{in}=0.0125 and given in Figure 6(a). It can be seen that higher α and Q resulted in lower Nu_D for the complete β set both in the choked and un-choked nozzle conditions, which can be attributed to the lower M, U and $\dot{m}$ values in the narrower nozzles with higher heat flux values as discussed through Figure 3(a). The augmentation in Nu_D towards downstream is an accompanied outcome of flow acceleration, and the ratio of the exit to inlet Nusselt numbers $\lambda=(Nu_D)_{ex}/(Nu_D)_{in}$ increase with β and α whereas decrease with Q. These findings agree well with those of Bartz [15], who reported augmented λ ratios with sharper α and with higher β, also with the λ=3.9 record of Ahmad [14] for a nozzle with $\alpha=45^o$. However Back et al.'s [13] λ of 1.61 for $\alpha=15^o$ conflicts with the current predictions, where the most significant ratio of λ=2.70 is evaluated for the choking case of $\alpha=9^o$. Due to the application of different heat flux values, Nu_D vary by ±7.9% (at the inlet) and ±6.5% (at the exit) for β=2 case within the complete α set whereas the corresponding intervals expand to ±8.8% and ±13.9% for β=1.25. The limits indicate that the effect of Q on Nu_D becomes more significant in lower β cases, thus in low Mach number flows.

Effects of ε on the streamwise Nu_D variations, for Q of 2000 kW/m^2, are investigated by the application of 3 different ε/D_{in} values of 0.0025, 0.025 and 0.05 and discussed by Figure 6(b). The resistive effect of ε on flow decreased Nu_D for all β and α cases. For the choked flow (β=2) the impact is more significant especially for the $\alpha=0^o$ nozzle with a variation of ±2.40% at the inlet, however the gap among the curves reduces towards downstream for each α set and at the exit Nu_D are in the neighborhood of ±0.35%. In the un-choked case (β=1.25) the inlet and exit Nu_D are within the range of ±1.37% and ±1.32% respectively, being closer at the inlet but separated at the exit than those of the choked case. The lower inlet velocities can explain the inlet closeness of Nu_D, whereas the enlargement of the exit range is due that the exit Mach numbers are not unique, as in the case of choked flow, but in the limit of ±3.92%, being the cause of the increase.

4. CONCLUSIONS

The effects of surface roughness and heat flux conditions on compressible converging-nozzle flows are investigated for various flow geometries and with different inlet and boundary conditions by means of a recently developed numerical model. The model is validated with the available numerical and experimental data from the literature and the main findings through the computational outputs can be summarized as follows:

- Both surface roughness and heat flux produce lower Mach numbers, moreover the effect of heat flux on the Mach number pattern is more apparent with lower nozzle convergence half angles.
- Upstream shear stress values decreased with lower inlet stagnation pressures, higher convergence half angles and heat flux conditions. However towards downstream, the shear stress values of the higher nozzle convergence half angle flows exceed those with smaller convergence half angles, and the intersection area of the shear stress values moves downstream with higher inlet stagnation pressures.
- Discharge coefficients increase with higher inlet stagnation pressures and with lower convergence half angles, surface roughness and heat flux conditions, where the effect of roughness is more remarkable in lower inlet stagnation pressure cases.
- Nusselt numbers decrease with lower inlet stagnation pressures and with higher convergence half angles, surface roughness and heat flux conditions. As the effect of surface heat flux, on Nusselt numbers, is more apparent in un-choked flows, the role of surface roughness becomes more significant in the choked flow with lower convergence half angles.

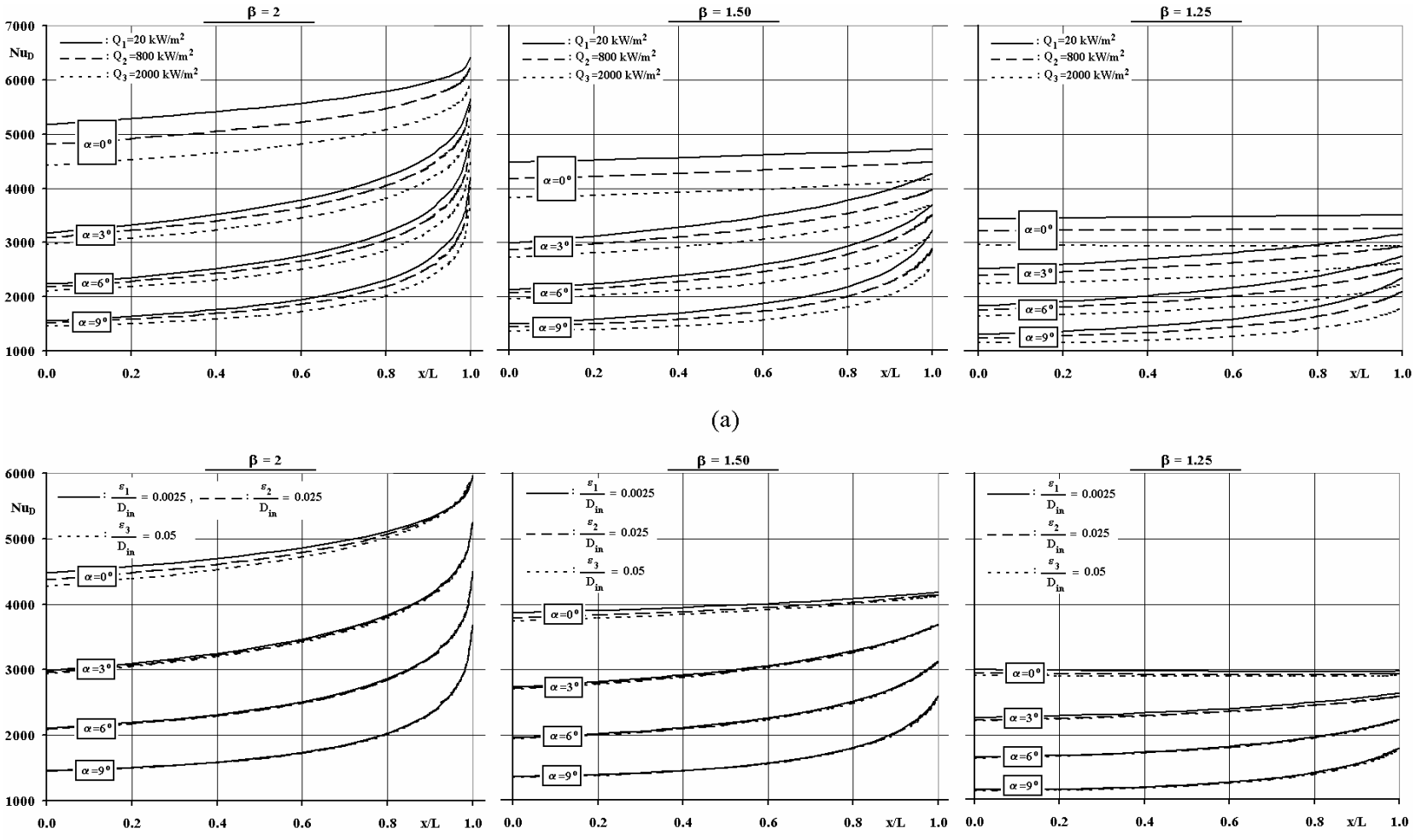

Figure 6. Influence of (a) constant heat flux and (b) surface roughness conditions on streamwise Nusselt number variations.

5. REFERENCES

1. Kammash, T. and Godfroy, T., An open cycle gas core fusion rocket for space exploration, Acta Astronautica, vol:41, 1997, pp.229-237.

2. Vargas, J.V.C. and Bejan, A., Thermodynamic optimization of finned crossflow heat exchangers for aircraft environmental control systems, Int. J. Heat Fluid Flow, vol:22, 2001, pp.657-665.

3. Assovskii, I.G., and Rashkovskii, S.A., Low-frequency instability of solid rocket motors: influence of the Mach effect and charge geometry, Combustion, Explosion and Shock Waves, vol:37, 2001, pp.321-330.

4. Massier, P.F., Back, L.H., Noel, M.B. and Saheli, F., Viscous effects on the flow coefficient for supersonic nozzle, AIAA Journal, vol:8, 1970, pp.605-607.

5. Krueger, P.S. and Gharib, M., The significance of vortex ring formation to the impulse and thrust of a starting jet, Physics of Fluids, vol:15, 2003, pp.1271-1281.

6. Park, K.A., Choi, Y.M., Choi, H.M., Cha, T.S. and Yoon, B.H., The evaluation of critical pressure ratios of sonic nozzles at low Reynolds numbers, Flow Measurement and Instrumentation, vol:12, 2001, pp.37-41.

7. Kim, H.D., Kim, J.H., Park, K.A., Setoguchi, T. and Matsuo, S., Computational study of the gas flow through a critical nozzle, Proc. Instn. Mech. Engrs. Part C: J. Mechanical Engineering Science, vol:217, 2003, pp.1179-1189.

8. Paik, J.S., Park, K.A. and Park, J.T., Inter-laboratory comparison of sonic nozzles at KRISS, Flow Measurement and Instrumentation, vol:11, 2000, pp.339-344.

9. Lear, W.E., Sherif, S.A. and Langford, J.R., Efficiency and gas dynamics analysis of two-phase mixtures in supersonic nozzles with inter-phase heat transfer and slip, Acta Astronautica, vol:40, 1997, pp.701-706.

10. Ribault, C.L. and Friedrich, R., Investigation of transport equations for turbulent heat fluxes in compressible flows, Int. J. Heat Mass Transfer, vol:40, 1997, pp.2721-2738.

11. Orieux, S., Rossi, C. and Esteve, D., Compact model based on a lumped parameter approach for the prediction of solid propellant micro-rocket performance, Sensors and Actuators A-Physical, vol:101, 2002, pp.383-391.

12. Sato, T., Tanatusgu. N., Naruo, Y., Kashiwagi, T., Omi, J., Tomike, J. and Nishino, T., Development study on ATREX engine, Acta Astronautica, vol:47, 2000, pp.799-808.

13. Back, L.H., Massier, P.F. and Cuffel R.F., Some observations on reduction of turbulent boundary-layer heat transfer in nozzle, AIAA Journal, vol:4, 1996, pp.2226-2229.

14. Ahmad, R.A., Discharge coefficients and heat transfer for axisymmetric supersonic nozzles, Heat Transfer Engineering, vol:22, 2001, pp.40-61.

15. Bartz, D.R., A simple equation for rapid estimation of rocket nozzle convective heat transfer coefficients, Jet Propulsion, vol:27, 1957, pp.49-51.

16. Maisonneuve, Y., Ablation of solid-fuel booster nozzle materials, Aerospace Science and Technology, vol:4, 1997, pp.211-289.

17. Bussiere, M. and Mora, B., Ariane 5 booster nozzle: components description and dimensioning, Acta Astronautica, vol:34, 1994, pp.83-89.

18. Shipway, P.H., The effect of plume divergence on the spatial distribution and magnitude of wear in gas-blast erosion, Wear, vol:205, 1997, pp.169-177.

19. Kumar, R., Verma, A.P. and Lal, G.K., Nozzle wear during the flow of a gas-particle mixture, Wear, vol:91, 1983, pp.33-43.

20. Krishnan, P., Evans, T., Ballal, K. and Kemble, L. J., Scanning electron microscopic studies of new and used fan nozzles for agricultural sprayers, Applied Engineering in Agriculture, vol:20, 2004, pp.133-137.

21. Incropera, F.P. and De Witt, D.P., Fundamentals of Heat and Mass Transfer, 3rd Edition, John Wiley & Sons, 1990.

22. Chapra, S.C. and Canale, R.P., Numerical Methods for Engineers, 2nd Edition, McGraw Hill, Singapore, 1990.

23. Laney, C.B., Computational Gasdynamics, 1st Edition, Cambridge University Press, 1998.
24. Wu, J.S. and Tseng K.C., Analysis of micro-scale gas flows with pressure boundaries using direct simulation Monte Carlo method, Computers and Fluids, vol:30, 2001, pp.711-735.

NOMENCLATURE

A	cross sectional area, m^2
C_d	discharge coefficient, dimensionless
C_p	specific heat at constant pressure, J/kgK
D	nozzle diameter, mm
dq	cellular heat flux, W/m^2
f	skin friction factor, dimensionless
F_f	friction force, N
I	thrust, N
L	nozzle length, m
$\dot{m}$	mass flow rate, kg/s
M	Mach number, dimensionless
Nu_D	Nusselt number, dimensionless
P	pressure, Pa
Pr	Prandtl number, dimensionless
Q	surface heat flux, W/m^2
R	gas constant, J/kgK
Re_D	Reynolds number, dimensionless
T	temperature, K
U	air velocity, m/s
x	streamwise direction, m

Greek Letters

α	convergence half angle, deg
β	inlet stagnation to back pressure ratio, dimensionless
ε	surface roughness, mm
γ	specific heat ratio, dimensionless
ν	kinematic viscosity, m^2/s
ρ	density, kg/m^3
τ	shear stress, Pa

Subscripts

b, o	back, stagnation
D	diameter
ex, in	exit, inlet
i, n	node, cell number
s	heat transfer surface

Superscripts

T	temperature dependency
$\overline{}$	cellular average